2012

Magnetism of directly ordered Sm-Co clusters

Balamurugan Balasubramanian
University of Nebraska-Lincoln, balamurugan@unl.edu

Ralph Skomski
University of Nebraska-Lincoln, rskomski2@unl.edu

Xingzhong Li
University of Nebraska - Lincoln, xli2@unl.edu

George C. Hadjipanayis
University of Delaware, hadji@udel.edu

David J. Sellmyer
University of Nebraska-Lincoln, dsellmyer@unl.edu

Magnetism of directly ordered Sm-Co clusters

B. Balamurugan,[1,2,a)] R. Skomski,[1,2] X. Z. Li,[1,2] G. C. Hadjipanayis,[3] and D. J. Sellmyer[1,2]
[1]*Nebraska Center for Materials and Nanoscience, University of Nebraska, Lincoln, Nebraska 68588, USA*
[2]*Department of Physics and Astronomy, University of Nebraska, Lincoln, Nebraska 68588, USA*
[3]*Department of Physics and Astronomy, University of Delaware, Newark, Delaware 19716, USA*

(Presented 31 October 2011; received 21 September 2011; accepted 16 November 2011; published online 7 March 2012)

Sm-Co bulk alloys have shown superior permanent-magnet properties, but research on Sm-Co nanoparticles is challenging because of the need to control particle size, size-distribution, crystalline ordering, and phase purity. In the present study, a cluster-deposition method was used to produce Sm-Co nanoparticles having desired crystal structures without the requirement of subsequent high-temperature thermal annealing. Poorly crystallized $SmCo_5$ nanoparticles exhibit a low room-temperature coercivity of only 100 Oe, whereas crystalline $SmCo_5$ and Sm_2Co_{17} nanoparticles show room-temperature coercivities of 2000 and 750 Oe, respectively. The direct synthesis of Sm-Co nanoparticles having sizes of less than 10 nm and a high degree of atomic ordering is an important step toward creating nanoparticle building blocks for permanent-magnets and other significant applications. © *2012 American Institute of Physics*. [doi:10.1063/1.3677668]

Bulk Sm-Co alloys have long been valued in permanent magnetism, especially $SmCo_5$ and Sm_2Co_{17}, which crystallize in the hexagonal $CaCu_5$ and rhombohedral Th_2Zn_{17}-type structures, respectively.[1–3] These materials exhibit high room-temperature magnetic anisotropy constants (K_1), namely 22×10^7 ergs/cm^3 ($SmCo_5$) and 3×10^7 ergs/cm^3 (Sm_2Co_{17}), along with high Curie temperatures ($T_c > 1020$ K) and appreciable magnetic polarizations ($J_s > 10$ kG).[3,4] The research on Sm-Co nanoparticles is, however, challenged by the requirement of high-temperature annealing above 800 °C for alloy formation and crystalline ordering, which results in poor control of size, size-distribution, and phase purity.[5–8]

$SmCo_5$ and Sm_2Co_{17} nanoparticles have previously been prepared by surfactant-assisted ball milling of bulk Sm-Co alloys, but these nanoparticles show a very low room-temperature coercivity of $\leq$100 Oe and a substantial reduction of magnetization due to the presence of surfactants, incomplete ordering, and oxidation.[5] In addition, ball milling process induces strains and amorphorization and also leads to the decomposition of the Sm-rich $SmCo_5$ phase.[8] Low-temperature wet chemical polyol process at about 270 °C using Co and Sm metal precursors in the presence of tetraethylene glycol resulted in $SmCo_5$ nanoparticles of particle sizes less than 20 nm with room temperature coercivities in the range of 100 to 1500 Oe.[6,7] Recently, the reduction of Sm(III) and Co(II) salts in tetraethylene glycol has been found to yield predominant Co_2C phase with x-diffraction peaks similar to $SmCo_5$.[9,10] Our recent work on plasma-condensation-type cluster deposition, performed under high-vacuum conditions, has been shown to reduce rare-earth oxidation and to produce single-phase and crystalline YCo_5 and Y_2Co_{17} nanoparticles without any high-temperature thermal annealing.[11]

In the present study, Sm-Co nanoparticles with different stoichiometries, especially $SmCo_5$ and Sm_2Co_{17}, were produced using a cluster deposition. The experimental setup consists of a cluster-formation chamber having a direct current (DC) magnetron plasma-sputtering discharge with a water-cooled gas-aggregation tube and a deposition chamber, where the substrate is kept at room temperature.[11,12] An Sm-Co composite target was sputtered using a mixture of Ar and He as sputtering gases to form Sm-Co nanoparticles in the gas-aggregation chamber, which were extracted as a collimated beam traveling toward the substrate in the deposition chamber. The desired stoichiometry and crystalline ordering were directly obtained during the aggregation process by controlling the DC magnetron sputtering power ($P_{dc} = 100 - 200$ W), prior to deposition on suitable substrates. Sm-Co nanoparticles were deposited on single crystalline Si (001) substrates for SQUID magnetometer, energy dispersive x-ray analysis (EDX), and x-ray diffraction (XRD: Rigaku D/Max-B diffractometer, Cu Kα with $\lambda = 1.5418$ Å) studies and on carbon coated copper grids for transmission electron microscopy (TEM: JEOL 2010 with an acceleration voltage of 200 kV) measurement.

The compositions and crystal structures of as-produced Sm-Co nanoparticles deposited at different P_{dc} were evaluated using EDX and XRD measurements, respectively. EDX analysis yields compositions corresponding to $SmCo_5$ for $100 \leq P_{dc} \leq 160$ W and Sm_2Co_{17} for $180 \leq P_{dc} \leq 200$ W (not shown here). The crystalline ordering of these nanoparticles also strongly depends on P_{dc}, as shown in the XRD patterns of Fig. 1, which include the standard positions and relative intensities of diffraction peaks corresponding to hexagonal $CaCu_5$ (blue vertical-solid lines) and rhombohedral Th_2Zn_{17}-type (red vertical-dotted lines).[13,14] Note that the maximum intensity diffraction peak corresponding to both the structures appears at angles of $2\theta = 39^\circ - 45^\circ$as revealed by the standard data.

a)Author to whom correspondence should be addressed. Electronic mail: bbalasubramanian2@unl.edu.

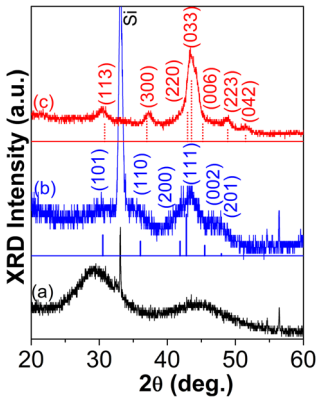

FIG. 1. (Color online) XRD patterns of Sm-Co nanoparticles prepared at different sputtering powers (P_{dc}): (a) $SmCo_5$ ($P_{dc} = 100$ W), (b) $SmCo_5$ ($P_{dc} = 160$ W), and (c) Sm_2Co_{17} ($P_{dc} = 200$ W). The standard peak positions corresponding to the hexagonal $CaCu_5$ (blue solid-vertical lines) and rhombohedral Th_2Zn_{17} (red dotted-vertical lines) structures are also given.

The XRD pattern of the as-produced $SmCo_5$ nanoparticles deposited at a low P_{dc} of 100 W shows only a broad and weak diffraction peak in the higher-angle region, along with another broad peak in the lower-angle region ($2\theta = 23° - 36°$), and thus reveals a poor crystalline ordering in these nanoparticles, as noted in Fig. 1(a). On increasing $P_{dc} = 160$ W, the diffraction peaks corresponding to $CaCu_5$ become visible and intense at higher angles, as noted in Fig. 1(b), revealing the improvement in the crystalline ordering. However, the XRD pattern of as-produced Sm_2Co_{17} nanoparticles deposited at a high P_{dc} of 200 W has intense and sharp diffraction peaks, which are in good agreement with the standard diffraction lines corresponding to the rhombohedral Th_2Zn_{17}-type structure, as noted in Fig. 1(c).

Note that some of the diffraction peaks separated by only a small angular position are indistinguishable, Figs. 1(b) and 1(c), because they have broad peaks resulting from their nanoparticle nature. The average particle size and size distribution of the Sm-Co nanoparticles were investigated using TEM. For example, the TEM micrograph of Fig. 2(a) and the corresponding particle-size histogram of $SmCo_5$ nanoparticles prepared at $P_{dc} = 160$ W exhibit an average particle size (d in Fig. 2(a)) of 8.4 nm and an rms standard deviation of $\alpha/d \simeq 0.20$. Sm_2Co_{17} nanoparticles deposited at a high power of 200 W exhibit an average particle size $d \simeq 10.8$ nm with $\alpha/d \simeq 0.19$ (Fig. 2(b)).

This study revealed a direct crystalline ordering of Sm-Co nanoparticles during the cluster-aggregation process by varying P_{dc} without subsequent high-temperature thermal annealing. However, Sm-Co intermetallics are characterized by small enthalpy differences per atom, as exemplified by $SmCo_5$ (−6.8 kJ/mol) and Sm_2Co_{17} (−8.0 kJ/mol), and require a complicated heat treatment for alloy formation and crystalization.[15] In the present study, a high $P_{dc} \geq 160$ W is expected to result in highly energetic and dense ions in the gas aggregation region, which leads to an increase in cluster-ion collision probability and subsequently provides sufficient energy for crystallization.[16]

The magnetic properties of Sm-Co nanoparticles were investigated by measuring the magnetization M as a function

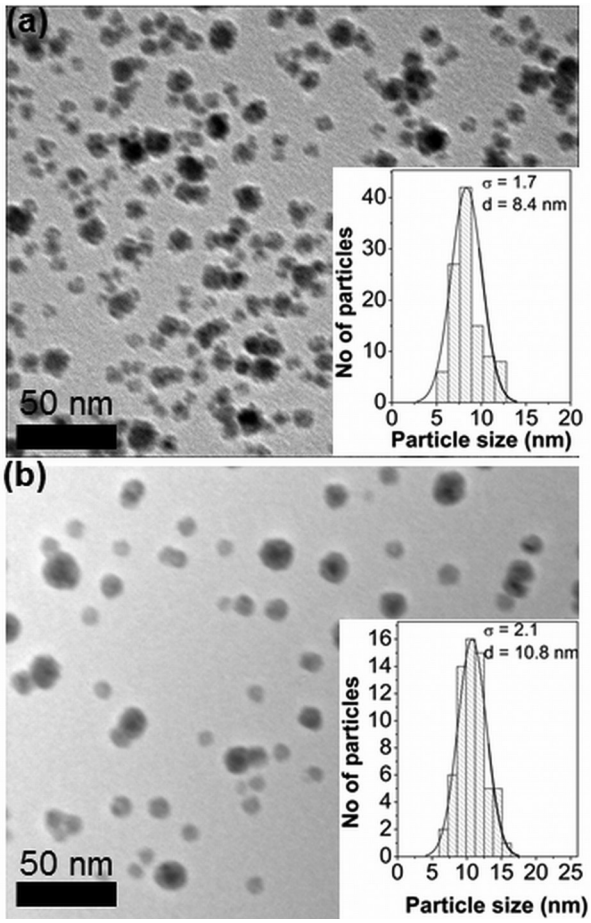

FIG. 2. Transmission electron microscope images of the cluster-deposited (a) $SmCo_5$ and (b) Sm_2Co_{17} nanoparticles, whereas the corresponding particle size histograms are given as an inset. σ and d are the standard deviation and average particle size, respectively.

of applied magnetic field H at 300 and 10 K. Figure 3 shows room-temperature hysteresis loops for Sm-Co nanoparticles prepared at different P_{dc}. Poorly crystalline $SmCo_5$ nanoparticles prepared at $P_{dc} = 100$ W exhibit a very low coercivity (H_c) of 100 Oe and a remanence ratio of $M_r/M_s = 0.23$ at 300 K, as noted in Fig. 3(a), where M_r and M_s are the remanent and saturation magnetizations, respectively. The soft-magnetic behavior in these nanoparticles is caused by reduced magnetocrystalline anisotropy due to the poor crystallinity.

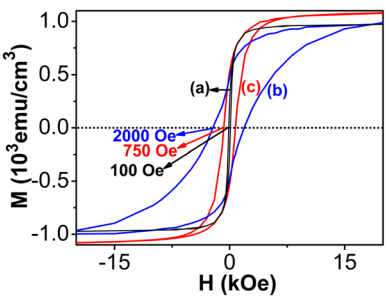

FIG. 3. (Color online) Room-temperature hysteresis loops for (a) poorly crystallized $SmCo_5$, (b) crystalline $SmCo_5$ and (c) crystalline Sm_2Co_{17} nanoparticles prepared at different sputtering powers of 100, 160, and 200 W, respectively.

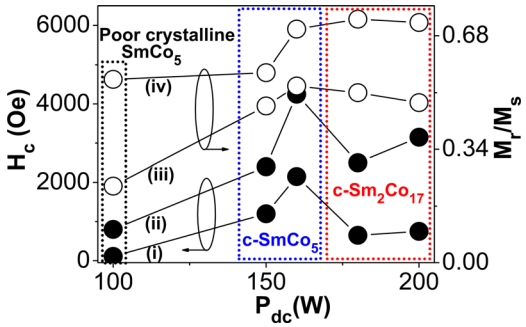

FIG. 4. (Color online) Magnetic properties of Sm-Co nanoparticles as a function of DC magnetron sputtering power P_{dc}: Coercivities (H_c) at (i) 300 K and (ii) 10 K and remanence ratios (M_r/M_s) at (iii) 300 and (iv) 10 K.

Crystalline $SmCo_5$ nanoparticles deposited at $P_{dc} = 160$ W exhibit hard-magnetic properties with $H_c = 2000$ Oe and $M_r/M_s = 0.53$ at 300 K, as noted in Fig. 3(b). Crystalline Sm_2Co_{17} nanoparticles deposited at a large $P_{dc} = 200$ W are softer, with $H_c = 750$ Oe and $M_r/M_s = 0.48$, as presented in Fig. 3(c). This can be attributed to the anisotropy constant of Sm_2Co_{17}, which is one order smaller than that of $SmCo_5$.[3] Fig. 3 also shows that crystalline $SmCo_5$ and Sm_2Co_{17} nanoparticles exhibit high J_s of 11.1 and 13.8 kG, respectively, which is similar to bulk. As summarized in Fig. 4, the magnetic properties of cluster-deposited Sm-Co nanoparticles measured at 300 and 10 K strongly depend on P_{dc}. H_c and M_r/M_s of Sm-Co nanoparticles are enhanced at 10 K as shown in Fig. 4.

Sm-Co nanostructures are known to exhibit a strong dependence of room-temperature coercivity on particle size.[8,17] H_c reaches a maximum value for a critical particle size and a further decrease in size leads to a decrease in H_c. This behavior has been attributed due to complex effects of crystalline ordering, surface morphology, and size-induced thermal fluctuations.[8,17,18] Note that room-temperature coercivities of crystalline $SmCo_5$ and Sm_2Co_{17} nanoparticles are in good agreement with the previously reported size-effects on the coercivity of Sm-Co.[8,17]

In conclusion, crystalline $SmCo_5$ and Sm_2Co_{17} nanoparticles were directly produced using a plasma-condensation-type cluster-deposition method without subsequent high-temperature thermal annealing. The Sm-Co nanoparticles gain sufficient energy from the inert gas ions during the gas-aggregation process for crystallization. $SmCo_5$ nanoparticles show comparatively hard magnetic properties with coercivities of 2000 and 4250 Oe at 300 and 10 K, respectively. The direct ordering of Sm-Co nanoparticles prior to deposition is important for assembling nanoparticle building blocks for practical applications.

ACKNOWLEDGMENTS

This work is supported by US Department of Energy (Grant No. DE-FG02-04ER46152, D.J.S., Advanced Research Projects Agency-Energy (Grant No. DE-AR 0000046, B.B. and G.C.H.), NSF-Materials Research Science and Engineering Center (Grant # DMR-0820521, R.S.), and Nebraska Center for Materials and Nanoscience (X.Z.L). Thanks are due to Zhiquang Sun for his technical assistance and Shah R. Valloppilly and Bhaskar Das for helpful discussions.

[1]K. Strnat, G. Hoffer, J. Olson, W. Ostertag, and J. J. Becker, J. Appl. Phys. **38**, 1001 (1967).
[2]M. Yue, J. H. Zuo, W. Q. Liu, W. C. Lv, D. T. Zhang, J. X. Zhang, Z. H. Guo, and W. Li, J. Appl. Phys. **109**, 07A711 (2011).
[3]R. Skomski, J. Phys. : Condens. Matter. **15**, R841 (2003).
[4]J. Sayama, K. Mizutani, T. Asahi, and T. Osaka, Appl. Phys. Lett. **85**, 5640 (2004).
[5]V. M. Chakka, B. Altuncevahir, Z. Q. Jin, and J. P. Liu, J. Appl. Phys. **99**, 08E912 (2006).
[6]T. Matsushita, T. Iwamoto, M. Inokuchi, and N. Toshima, Nanotechnology **21**, 095603 (2010).
[7]P. Saravanan, G. V. Ramana, K. S. Rao, B. Sreedhar, V. T. P. Vinod, and V. Chandrasekaran, J. Magn. Magn. Mater. **323**, 2083 (2011).
[8]N. Poudyal, C. Rong, and J. P. Liu, J. Appl. Phys. **107**, 09A703 (2011).
[9]C. N. Chinnasamy, J. Y. Huang, L. H. Lewis, B. Latha, C. Vittoria, and V. G. Harris, Appl. Phys. Lett. **93**, 032505 (2008).
[10]C. N. Chinnasamy, J. Y. Huang, L. H. Lewis, B. Latha, C. Vittoria, and V. G. Harris, Appl. Phys. Lett. **97**, 059901 (2010).
[11]B. Balasubramanian, R. Skomski, X. Z. Li, S. R. Valloppilly, J. E. Shield, G. C. Hadjipanayis, and D. J. Sellmyer, Nano Lett. **11**, 1747 (2011).
[12]B. Balamurugan, R. Skomski, and D. J. Sellmyer, *Magnetic Clusters and Nanoparticles in Nanoparticles: Synthesis, Characterization, and Applications*, edited by R. S. Chaughule and R. V. Ramanujan (American Scientific Publishers, California, 2010) p. 127.
[13]ICDD- 2011 International Centre for Diffraction Data, Card No. 01-075-2837.
[14]ICDD- 2011 International Centre for Diffraction Data, Card No. 04-001-1105.
[15]F. Meyer-Liautaud, C. H. Allibert, and R. Castanet, J. Less-Common Met. **127**, 243 (1987).
[16]M. M. Patterson, A. Cochran, J. Ferina, X. Rui, T. A. Zimmerman, Z. Sun, D. J. Sellmyer, and J. E. Shield, J. Vac. Sci. Technol. B **28**, 273 (2010).
[17]C. H. Chen, S. J. Knutson, Y. Shen, R. A. Wheeler, J. C. Horwath, and P. N. Barnes, Appl. Phys. Lett. **99**, 012504 (2010).
[18]E. F. Kneller and F. E. Luborsky, J. Appl. Phys. **34**, 656 (1963).